*Inorg. Chem.* **2006**, *45*, 4728–4734


# Triiodide Quenching of Ruthenium MLCT Excited State in Solution and on $TiO_2$ Surfaces: An Alternate Pathway for Charge Recombination

**Christopher C. Clark, Andras Marton, Ramya Srinivasan, Amy A. Narducci Sarjeant, and Gerald J. Meyer***

*Departments of Chemistry and Materials Science and Engineering, Johns Hopkins University, Baltimore, Maryland 21218*

Received February 13, 2006

The excited states of $[Ru(bpy)_2(deeb)](PF_6)_2$, where bpy is 2,2-bipyridine and deeb is 4,4′-$(CO_2CH_2CH_3)_2$-2,2′-bipyridine, were found to be efficiently quenched by triiodide ($I_3^-$) in acetonitrile and dichloromethane. In dichloromethane, $I_3^-$ was found to quench the excited states by static and dynamic mechanisms; Stern–Volmer analysis of the time-resolved and steady-state photoluminescence data produced self-consistent estimates for the $I_3^- + Ru(bpy)_2(deeb)^{2+} \rightleftarrows [Ru^{II}(bpy)_2(deeb)^{2+},(I_3^-)]^+$ equilibrium, $K = 51{,}000\ M^{-1}$, and the bimolecular quenching rate constant, $k_q = 4.0 \times 10^{10}\ M^{-1}\ s^{-1}$. In acetonitrile, there was no evidence for ion pairing and a dynamic quenching rate constant of $k_q = 4.7 \times 10^{10}\ M^{-1}\ s^{-1}$ was calculated. Comparative studies with $Ru(bpy)_2(deeb)^{2+}$ anchored to mesoporous nanocrystalline $TiO_2$ thin films also showed efficient excited-state dynamic quenching by $I_3^-$ in both acetonitrile and dichloromethane, $k_q = 1.8 \times 10^9$ and $3.6 \times 10^{10}\ M^{-1}\ s^{-1}$, respectively. No reaction products for the excited-state quenching processes were observed by nanosecond transient absorption measurements from 350 to 800 nm under any experimental conditions. X-ray crystallographic, IR, and Raman data gave evidence for interactions between $I_3^-$ and the bpy and deeb ligands in the solid state.

## Introduction

Dye-sensitized solar cells (DSSCs) have received widespread attention as efficient low-cost alternatives to silicon photovoltaics.[1,2] The most efficient DSSCs are based on mesoporous nanocrystalline $TiO_2$ thin films with Ru(II) polypryidyl compounds as sensitizers. An organic electrolyte that contains triiodide−iodide ($I_3^-/I^-$) redox mediators and a platinum counter electrode complete the cell. Upon light absorption by the sensitizer, excited-state electron injection into the $TiO_2$ nanocrystallites occurs. The redox mediator then regenerates the oxidized sensitizer and transports the charge through the mesoporous film to the Pt electrode where it is reduced. Although absorbed photon-to-current efficiencies are often near unity with $I_3^-/I^-$ mediators, even the most efficient DSSCs convert only about half of the excited-state energy into photovoltage.[1,2] Attempts to circumvent this problem with alternative mediators have met only limited success.[3−6] Thus far, $I_3^-/I^-$ redox mediators seem to offer the unique ability to rapidly regenerate the sensitizer and transport charge between the electrodes without significant recombination losses.

The redox properties of $I^-$ and $I_3^-$ can potentially lead to quenching of sensitizer excited states prior to electron injection into the semiconductor nanoparticle.[7] Such processes may be particularly important for sensitizers that are remote to or those held at a fixed distance from the semiconductor surface.[8,9] Previous studies with metal-to-ligand charge transfer (MLCT) excited states have focused mainly on iodide. As first demonstrated by Lever,[10] electron-transfer quenching requires a potent photooxidant because of the very positive aqueous reduction potential, $E(I^{\bullet/-}) = +1.3$ V vs SCE.[7] More recently it has been shown that ion

* To whom correspondence should be addressed. E-mail: meyer@jhu.edu.

(1) O'Regan, B.; Gratzel, M. *Nature* **1991**, *353*, 737−740.
(2) Vlachopoulos, N.; Liska, P.; Augustynski, J.; Gratzel, M. *J. Am. Chem. Soc.* **1988**, *110*, 1216−1220.
(3) Oskam, G.; Bergeron, B. V.; Meyer, G. J.; Searson, P. C. *J. Phys. Chem. B* **2001**, *105*, 6867−6873.
(4) Gregg, B. A.; Pichot, F.; Ferrere, S.; Fields, C. L. *J. Phys. Chem. B* **2001**, *105*, 1422−1429.
(5) Argazzi, R.; Bignozzi, C. A.; Heimer, T. A.; Castellano, F. N.; Meyer, G. J. *J. Phys. Chem. B* **1997**, *101*, 2591−2597.
(6) Sapp, S. A.; Elliott, C. M.; Contado, C.; Caramori, S.; Bignozzi, C. A. *J. Am. Chem. Soc.* **2002**, *124*, 11215−11222.
(7) Stanbury, D. M. *Adv. Inorg. Chem.* **1989**, *33*, 69.
(8) Liu, F.; Meyer, G. J. *Inorg. Chem.* **2005**, *44*, 9305−9313.
(9) Galoppini, E.; Guo, W. Z.; Zhang, W.; Hoertz, P. G.; Qu, P.; Meyer, G. J. *J. Am. Chem. Soc.* **2002**, *124*, 7801−7811.
(10) Haga, M. A.; Dodsworth, E. S.; Eryavec, G.; Seymour, P.; Lever, A. B. P. *Inorg. Chem.* **1985**, *24*, 1901−1906.



10.1021/ic060246q CCC: $33.50 © 2006 American Chemical Society
Published on Web 05/16/2006

**Scheme 1.** Simplified Energy Level Diagram of a Sensitized $TiO_2$ Interface that Shows Back Electron Transfer (1) and Excited State Quenching (2) with $I_3^-$

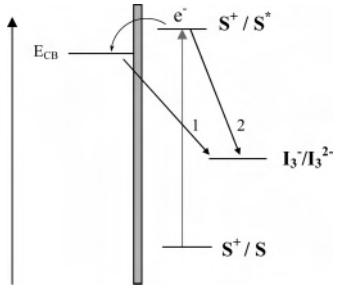


pairing in nonaqueous solutions,[11] and perhaps at metal oxide interfaces,[12,13] can make the process more favorable for weak excited-state oxidants. Much less is known about how triiodide might interact with MLCT excited states.

Hupp and co-workers have recently reported evidence for excited-state electron transfer from porphyrin sensitizers to $I_3^-$ that can, under certain conditions, result in a reverse (cathodic) photocurrent.[14] Back electron transfer from $TiO_2$ to $I_3^-$ is also commonly invoked to explain the low photovoltages observed in DSSCs.[2,15] The number of electrons that recombine by this pathway is necessarily small as the absorbed photon-to-current efficiency of the most efficient DSSCs are within the experimental uncertainty of unity. However, the small fraction that recombine by this pathway are thought to have a significant impact on the semiconductor quasi-Fermi level and hence the measured photovoltage. The possible electron-transfer pathways to $I_3^-$ at sensitized interfaces are shown in Scheme 1.

In this paper, we provide experimental conditions for efficient quenching of MLCT excited states by $I_3^-$. Spectroscopic evidence for both static and dynamic quenching mechanisms allowed the equilibrium and quenching constants to be quantified in fluid solution. Comparative studies were performed with sensitizers anchored to nanocrystalline $TiO_2$ where the static mechanism was found to be absent.

## Experimental Section

**Materials.** Tetrabutylammonium triiodide, $TBAI_3$ (Fluka), tetrabutylammonium hexafluorophosphate, TBAH (Aldrich), dichloromethane (HPLC grade, EMD), acetonitrile (Burdick and Jackson), and ethyl ether (Fischer) were all used as received. Samples of $[Ru(bpy)_2(deeb)](PF_6)_2$ were available from previous studies.[11] Mesoporous nanocrystalline $TiO_2$ films deposited on glass slides were prepared as previously described.[16] Prior to sensitzer binding the films were pretreated with aqueous pH 11 solutions as previously described.[17] The $Ru(bpy)_2(deeb)^{2+}$ sensitizer was anchored to the $TiO_2$ nanoparticles by overnight reactions in acetonitrile and are abbreviated at $Ru^{2+}/TiO_2$.

**Spectroscopy. Photoluminescense.** Steady-state photoluminescence (PL) spectra were obtained with a Spex Fluorolog that had been calibrated with a certified lamp. Samples of $[Ru(bpy)_2(deeb)](PF_6)_2$ in dichloromethane and acetonitrile were purged with $N_2$ gas for 20 min. PL spectra were taken with 500 nm excitation. Time-resolved PL data in solution were obtained with the same setup as for the transient absorption experiments (see below). For surface studies, $Ru^{2+}/TiO_2$ thin films were placed flush against one face of a 1 cm quartz cuvette with the sensitized film facing towards the solution. Measurements were made in front-face mode.

**UV−vis Absorbance.** All UV−vis absorption data were obtained on a Varian Cary 50 UV−vis spectrophotometer in a 1 cm square quartz cuvette at room temperature.

**Transient Absorbance.** Transient absorption spectra were obtained as described earlier.[11] In short, pulsed 532.5 nm light (8−10 ns fwhm, 2.5 mJ/pulse) from a Surelite II Nd:YAG, Q-switched laser was used as the excitation source. A homogeneous portion of the laser was selected using an iris and then expanded to approximately 1 $cm^2$ using a quartz concave lens. The sample was probed at a right angle with a 150 W pulsed Xe lamp (Applied Photophysics). Each kinetic trace was acquired as an average of 40−200 laser shots at 1 Hz repetition rate. Samples were prepared in a 1 cm square quartz cuvette and purged with nitrogen gas for 20 min. Absorption spectra were recorded before and after transient absorption experiments.

**IR.** Infrared spectra of all samples were acquired on a Nexus 670 FT-IR equipped with a Smart Golden Gate attenuated total reflectance (ATR) accessory from Thermo Nicolet. Samples were acquired at 1, 2, and 4 $cm^{-1}$ resolution. At the highest resolution, sharp peaks from the diamond ATR accessory were observed that could not be fully subtracted. For this reason, the data presented here were obtained at 4 $cm^{-1}$ resolution.

**Raman.** FT-Raman spectra were obtained with the Raman module of a Nexus 670 FT-IR equipped with a Nd:YAG laser (1064 nm) and a liquid nitrogen cooled InGaAs detector. Spectra were an average of 256 scans collected at a 1 $cm^{-1}$ resolution. A laser power of 1 W was used.

**X-ray Crystallography.** Crystals of $[Ru(bpy)_2(deeb)](I_3)_2$ were grown by addition of a 10-fold molar excess of tetrabutylammonium triiodide to $[Ru(bpy)_2(deeb)](PF_6)_2$ in $CH_2Cl_2$. The solution was placed in an open vial inside a diethyl ether filled vapor chamber. Dark red-orange crystals formed within 3 days. A suitable crystal of $[Ru(bpy)_2(deeb)](I_3)_2$ was mounted in oil on the end of a glass fiber and used for X-ray crystallographic analysis. The X-ray intensity data were measured at 110 K on an Oxford Diffraction Xcalibur3 system equipped with a graphite monochromator and a CCD detector. The final cell was obtained through a refinement of 8988 reflections to a maximum resolution of 0.57 Å. Data were collected via a series of 1.0° $\varphi$ and $\omega$ scans. The frames were integrated with the Oxford Diffraction CrysAlisRED software package. A face-indexed absorption correction and an interframe scaling correction were also applied. The structure was solved using direct methods and refined using the Bruker SHELXTL (version 6.1) software package. Analysis of the data showed no sample decomposition.

## Results

Figure 1 shows the absorption spectra of $[Ru(bpy)_2(deeb)](PF_6)_2$ in dichloromethane. The Ru → bpy and Ru → deeb charge-transfer (CT) bands are not well resolved, but the

(11) Marton, A.; Clark, C. C.; Srinivasan, R.; Freundlich, R. E.; Narducci-Sarjeant, A. A.; Meyer, G. J. *Inorg. Chem.* **2006**, *45*, 362−369.
(12) Nasr, C.; Hotchandani, S.; Kamat, P. V. *J. Phys. Chem. B* **1998**, *102*, 4944−4951.
(13) Fitzmaurice, D. J.; Frei, H. *Langmuir* **1991**, *7*, 1129−1137.
(14) Splan, K. E.; Massari, A. M.; Hupp, J. T. *J. Phys. Chem. B* **2004**, *108*, 4111−4115.
(15) Zhang, Z. P.; Zakeeruddin, S. M.; O'Regan, B. C.; Humphry-Baker, R.; Gratzel, M. *J. Phys. Chem. B* **2005**, *109*, 21818−21824.
(16) Heimer, T. A.; Darcangelis, S. T.; Farzad, F.; Stipkala, J. M.; Meyer, G. J. *Inorg. Chem.* **1996**, *35*, 5319−5324.
(17) Qu, P.; Meyer, G. J. *Langmuir* **2001**, *17*, 6720−6728.

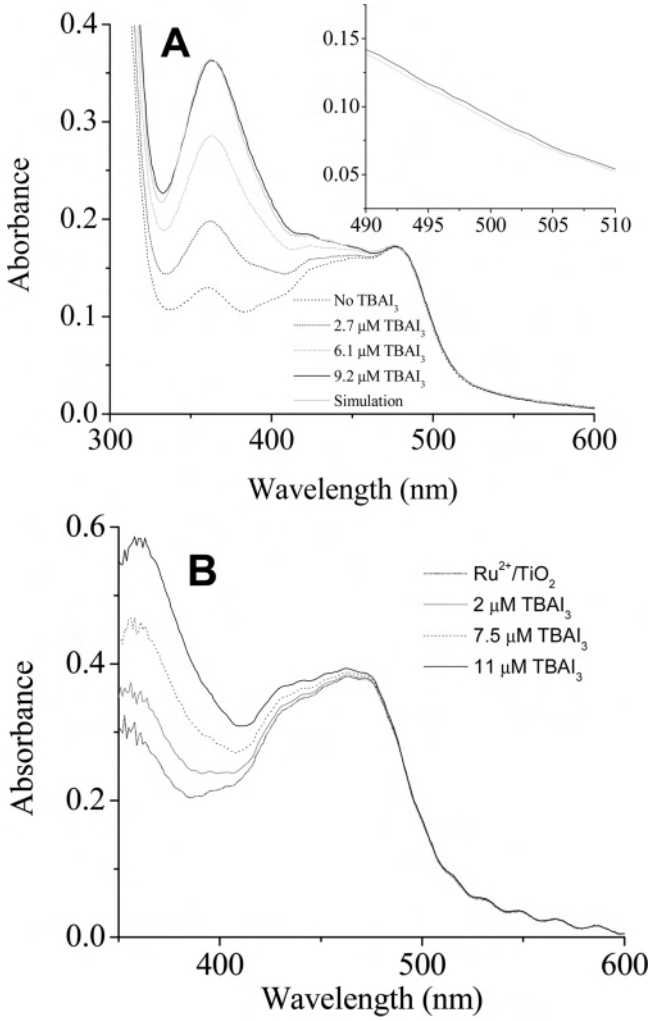


**Figure 1.** UV−vis absorption spectra of (A) $Ru(bpy)_2(deeb)^{2+}$ and (B) $Ru^{2+}/TiO2$ in $CH_2Cl_2$ with the indicated concentrations of $TBAI_3$. A simulated spectrum for the 9.2 $\mu$M $I_3^-$ data is overlaid. The inset in 1A shows an expanded region of the simulated and experimental data with 9.2 $\mu$M $I^{3-}$.

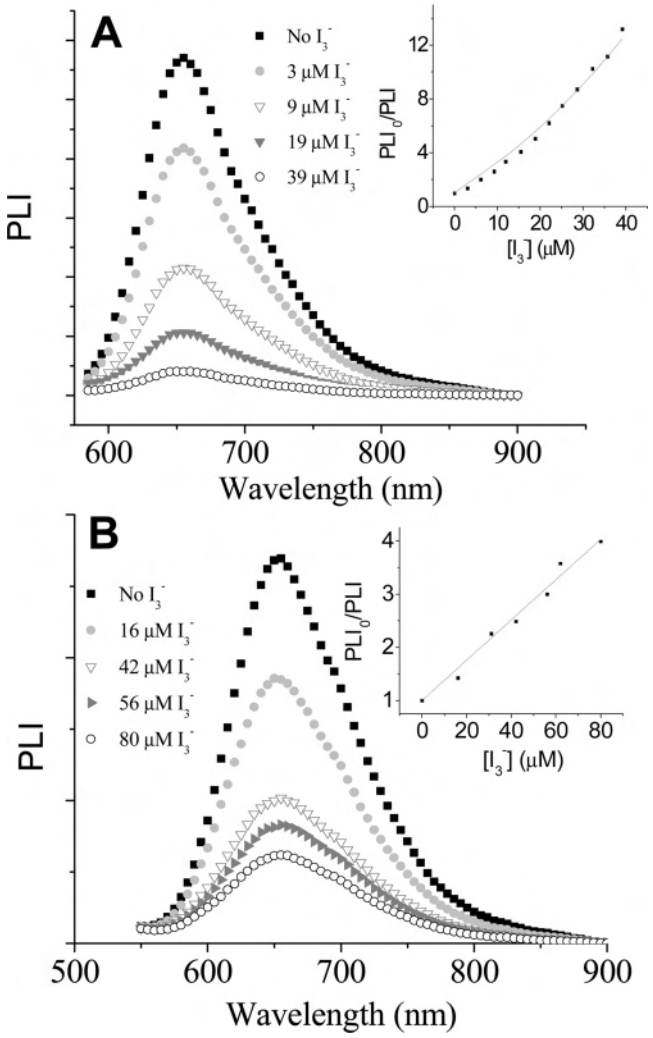


**Figure 2.** Room-temperature steady-state photoluminescence spectra of (A) $Ru(bpy)_2(deeb)^{2+}$ and (B) $Ru^{2+}/TiO_2$ in $CH_2Cl_2$ with the indicated $TBAI_3$ concentrations.

Ru → deeb CT band accounts for most of the oscillator strength at lower energies, $\lambda > 480$ nm.[18] The addition of $TBAI_3$ to the dichloromethane solution resulted in perturbations of the $Ru(bpy)_2(deeb)^{2+}$ spectrum. The changes to the MLCT bands were small and only quantifiable when the spectra were carefully compared to simulations created by standard addition of the $Ru(bpy)_2(deeb)^{2+}$ and $TBAI_3$ absorption spectra in dichloromethane to that of a slight red shift of the Ru → deeb CT band was observed on the low-energy side of the MLCT band that could not be reproduced in the simulations (∼500 nm, Figure 1 inset). A small red shift also occurred for the $I_3^-$ absorption band at 360 nm. Analogous experiments were carried out in acetonitrile solution where the absorption changes with $I_3^-$ addition could be modeled by the standard addition method.

Studies were performed where $Ru(bpy)_2(deeb)^{2+}$ was anchored to pH 11 pretreated $TiO_2$ thin films, abbreviated as $Ru^{2+}/TiO_2$, and immersed in $CH_2Cl_2$. When $TBAI_3$ was added to $Ru^{2+}/TiO_2$, no spectral changes of the MLCT absorption were observed. Likewise, the $Ru^{2+}/TiO_2$ absorption spectrum was not changed by the addition of $TBAI_3$ in acetonitrile, Figure 1B.

The steady-state photoluminescence intensity of $Ru(bpy)_2(deeb)^{2+}$* and $Ru^{2+}$*/$TiO_2$ in $CH_2Cl_2$ was quenched by the addition of $TBAI_3$, Figure 2. Stern−Volmer analysis of the solution data produced an upward curving plot, Figure 2A inset. Stern−Volmer plots for $Ru^{2+}$*/$TiO_2$ were linear, Figure 2B inset. The studies were repeated in acetonitrile where Stern−Volmer plots for both $Ru(bpy)_2(deeb)^{2+}$* and $Ru^{2+}$*/$TiO_2$ were linear, indicative of a purely dynamic quenching mechanism.[19]

Time-resolved photoluminescence studies were performed with $TBAI_3$ added to $CH_2Cl_2$ solutions of $Ru(bpy)_2(deeb)^{2+}$ and $Ru^{2+}/TiO_2$. Excited-state decay in fluid solution was well described by a first-order kinetic model (eq 1)

$$\mathrm{PLI}(t) = \alpha \exp[-(kt)] \qquad (1)$$

where α is the initial amplitude and $k$ represents the sum of

(18) Kelly, C. A.; Farzad, F.; Thompson, D. W.; Meyer, G. J. *Langmuir* **1999**, *15*, 731−737.

(19) Lakowicz, J. R. *Principles of Fluorescence Spectroscopy*, 2nd ed.; Kluwer Academic/Plenum Publishers: New York, 1999.

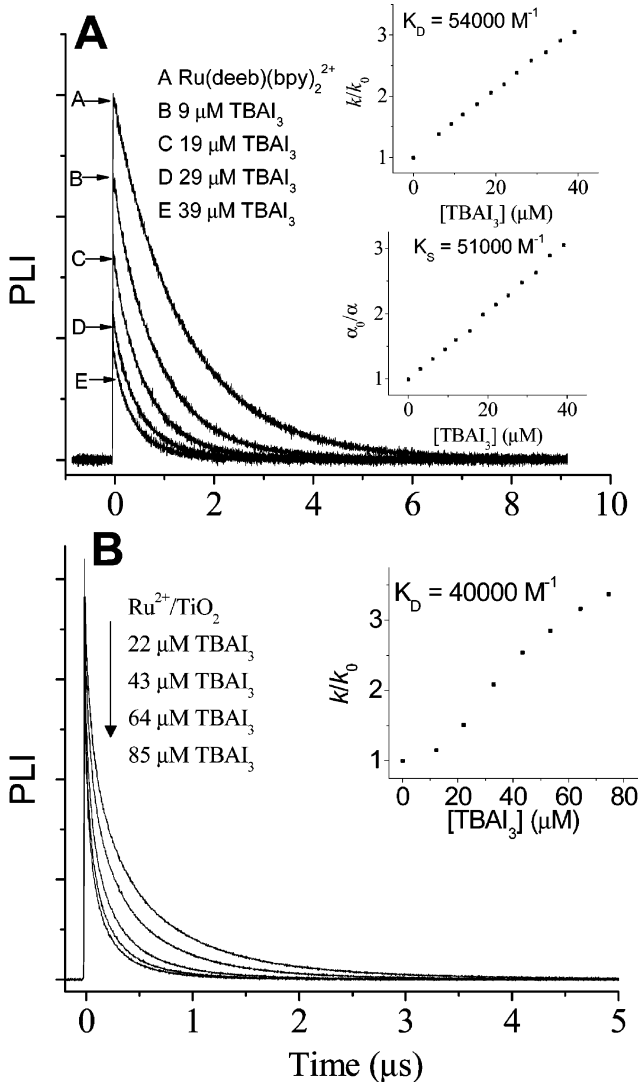


**Figure 3.** Room-temperature time-resolved photoluminescence spectra of (A) $Ru(bpy)_2(deeb)^{2+}$ and (B) of $Ru^{2+}/TiO_2$ in $CH_2Cl_2$ with the indicated $TBAI_3$ concentrations. The samples were excited with 532 nm light (3.5 mJ/pulse), and the photoluminescence was monitored at 650 and 610 nm for solution and surface, respectively.

the radiative and nonradiative rate constants. The addition of $TBAI_3$ was found to decrease α and increase $k$, consistent with both static and dynamic quenching mechanisms, respectively. Stern−Volmer analysis yielded a dynamic quenching rate constant, $k_q = K_D/\tau_0 = 4.0 \times 10^{10}$ $M^{-1}$ $s^{-1}$, where $\tau_0$ is the lifetime ($1/k$) in the absence of $I_3^-$. Similar analysis of the static component yielded an equilibrium constant of $K_s = 51\,000$ $M^{-1}$, Figure 3A. With 0.1 M tetrabutylammonium hexafluorophosphate, the static component was absent, and the quenching rate constant decreased to $4.0 \times 10^9$ $M^{-1}$ $s^{-1}$. Experiments performed in acetonitrile showed only dynamic quenching, and the Stern−Volmer analysis yielded $k_q = 4.7 \times 10^{10}$ $M^{-1}$ $s^{-1}$.

Excited-state decay for $Ru^{2+}*/TiO_2$ was nonexponential but was well described by a parallel first- and second-order kinetic model, eq 2.[20] Here, $A$ is a constant proportional to

$$\mathrm{PLI}(t) = \frac{A \times \exp[-(t/\tau)]}{\tau \times (1/\tau) + p - p \times \exp[-(t/\tau)]} \qquad (2)$$

**Table 1.** Quenching Constants in Acetonitrile and Dichloromethane[a]

| | $K_D$ ($M^{-1}$) | $K_S$ ($M^{-1}$) | $k_q$ ($M^{-1}$ $s^{-1}$) | $\tau_0$ (μs) |
|---|---|---|---|---|
| $Ru(bpy)_2(deeb)^{2+}/CH_2Cl_2$ | 54 000 | 51 000 | $4.0 \times 10^{10}$ | 1.36 |
| $Ru^{2+}/TiO_2$ in $CH_2Cl_2$ | 40 000 | | $3.6 \times 10^{10}$ | 1.13[b] |
| $Ru(bpy)_2(deeb)^{2+}/CH_3CN$ | 47 000 | | $4.7 \times 10^{10}$ | 0.990 |
| $Ru^{2+}/TiO_2$ in $CH_3CN$ | 1800 | | $1.8 \times 10^9$ | 0.960[b] |

[a] All measurements at room temperature. [b] Lifetimes extracted from a parallel first- and second-order kinetic analysis of the excited-state decay.

**Table 2.** Crystal Parameters for $Ru(bpy)_2(deeb)(I_3)_2$

| | |
|---|---|
| empirical formula | $C_{36}H_{32}I_6N_6O_5Ru$ |
| fw | 1475.15 |
| cryst color, habit | red-orange blade |
| temp | 110 K |
| radiation | Mo Kα ($\lambda = 0.71073$ Å) |
| space group | $P\bar{1}$ |
| unit cell dimensions | $a = 11.132(2)$ Å, $\alpha = 89.967(11)°$<br>$b = 12.4849(19)$ Å, $\beta = 84.388(12)°$<br>$c = 16.0516(19)$ Å, $\gamma = 84.775(14)°$<br>vol = 2210.8(6) Å$^3$ |
| $Z$ | 2 |
| calcd density | 2.216 Mg/m$^3$ |
| abs coeff | 4.58691 mm$^{-1}$ |
| $R(F)$ | 0.0575 |
| $R(wF^2)$ | 0.1659 |

the initial amplitude, $1/\tau$ is the first-order rate constant, and $p$ is the product of the second-order rate constant and the concentration of $Ru(bpy)_2(deeb)^{2+}*$ at $t = 0$.[20] The second-order component has been attributed to annihilation between two $Ru^{2+}/TiO_2$ MLCT excited states and has been discussed recently in some detail.[20] For $Ru^{2+}/TiO_2$ thin films immersed in dichloromethane, the addition of $TBAI_3$ was found to decrease the excited-state lifetime with no evidence for static quenching. Stern−Volmer analysis of the dynamic component yielded a bimolecular quenching rate constant on the same order of magnitude as that measured in fluid dichloromethane, $k_q = 3.6 \times 10^{10}$ $M^{-1}$ $s^{-1}$, Figure 3B. For $Ru^{2+}/TiO_2$ thin films immersed in acetonitrile, the rate of quenching by $I_3^-$ was significantly slower, $k_q = 1.8 \times 10^9$ $M^{-1}$ $s^{-1}$, and no quantifiable static component was observed, Figure 3B. The results of the Stern−Volmer analysis are summarized in Table 1.

Nanosecond time-resolved transient absorption studies with pulsed 532.5 nm light excitation were performed on a 20 μM solution of $Ru(bpy)_2(deeb)^{2+}$ with 50 μM $TBAI_3$ in $CH_2Cl_2$. Within the time resolution of our apparatus (~8 ns), no charge-transfer products were detected from 350 to 800 nm. The lifetime of the MLCT excited state was observed to decrease from 1.36 μs to 380 ns as a result of quenching by $I_3^-$. At higher $TBAI_3$ concentrations, the characteristic absorption spectrum of $I_2^{-\bullet}$ was transiently observed.[21] However, control experiments performed in the absence of $Ru(bpy)_2(deeb)^{2+}$ showed that this was the result of the direct excitation of $I_3^-$, as has been previously described.[22] Transient absorption studies with $Ru^{2+}/TiO_2$ and $I_3^-$ in $CH_2Cl_2$ also showed no evidence for charge-separated products.

A single crystal of $Ru(bpy)_2(deeb)\cdot(I_3)_2$ was characterized crystallographically, Table 2. A space filling model and an ORTEP diagram is displayed in Figure 4. The two triiodide

(20) Higgins, G. T.; Bergeron, B. V.; Hasselmann, G. M.; Farzad, F.; Meyer, G. J. *J. Phys. Chem. B* **2006**, *110*, 2598−2605.

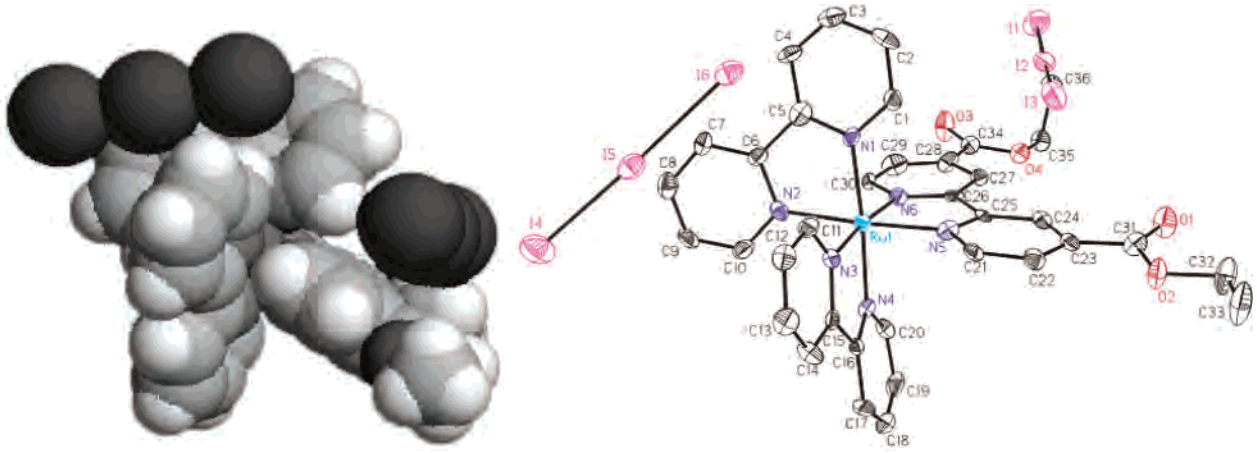

**Figure 4.** X-ray crystal structure of $Ru(bpy)_2(deeb)\cdot(I_3)_2$ (left, space-filling model; right, ORTEP diagram from a different view).

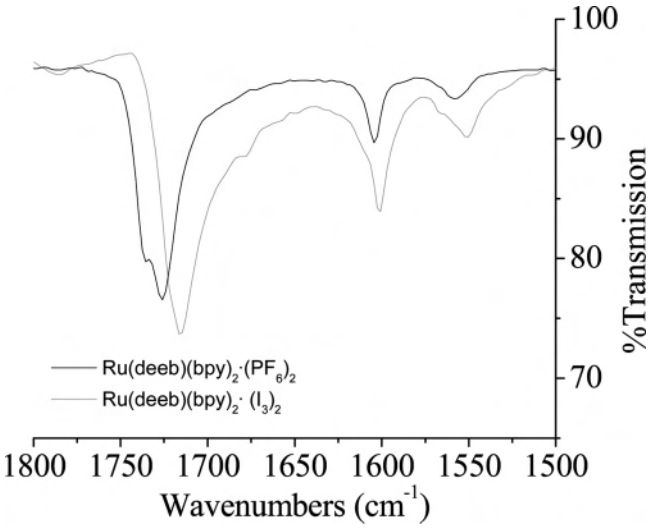


**Figure 5.** FT-IR spectra of $Ru(bpy)_2(deeb)\cdot(PF_6)_2$ (−) and $Ru(bpy)_2(deeb)\cdot(I_3)_2$ (−) single crystals, respectively.

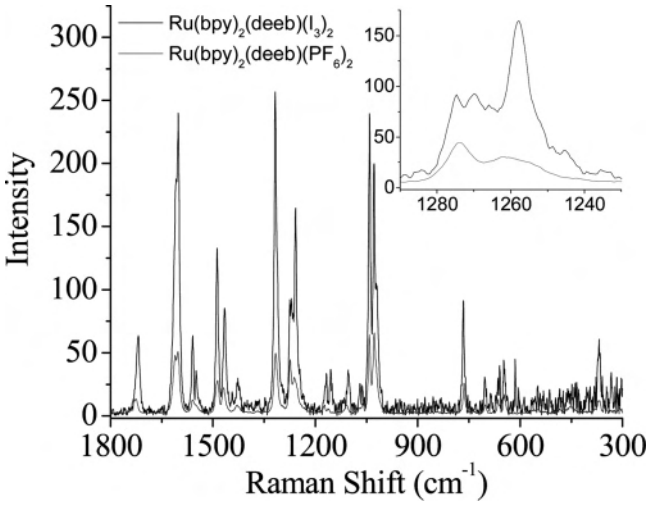


**Figure 6.** FT-Raman spectra of $Ru(bpy)_2(deeb)\cdot(I_3)_2$ and $Ru(bpy)_2(deeb)\cdot(PF_6)_2$ salts, respectively. The inset is an expansion of this same data.

anions were located on opposite sides of the Ru compound, with one located above the ethyl ester groups and the other between two adjacent bipyridine ligands. Every iodide in the two triiodide anions was within 4 Å of the bpy or deeb ligands. The angles between the ester linking groups and the bipyridine planes were found to be 7.6 and 13.1°, respectively.

Figures 5 and 6 show the IR and Raman spectra of the $Ru(bpy)_2(deeb)\cdot(I_3)_2$ and $Ru(bpy)_2(deeb)\cdot(PF_6)_2$ salts. While the asymmetric $\nu$(CO) stretch of the $PF_6^-$ salt (~1730 $cm^{-1}$) shows two distinctive stretches, the intensity of the higher-energy band was minimal for the $I_3^-$ salt. In addition, the $\nu$(CO) stretch was 12 $cm^{-1}$ (7 $cm^{-1}$) lower in energy in the IR (Raman) spectra of the $I_3^-$ salt. Raman spectroscopy data revealed distinct spectral changes evident in the bipyridine modes from 1200 to 1300 $cm^{-1}$.

## Discussion

X-ray crystallography provided evidence for solid-state adduct formation between $I_3^-$ and $Ru(bpy)_2(deeb)^{2+}$, as well as insights into how triiodide might interact with sensitizers at semiconductor interfaces. One $I_3^-$ anion was positioned parallel to the plane of the deeb ligand, with the nearest iodide about 3.97 Å away from the terminal methyl group. The other $I_3^-$ anion was located between the two bpy ligands, with the closest iodide lying 3.76 Å away from the adjacent pyridine ring. The interionic distance between the two $I_3^-$ molecules was 7.10 Å. We note that Elliot and Walters have also reported crystallographic evidence of ion pairing between $I_3^-$ and $Cr(4,4'\text{-}(CH_3)_2\text{-bpy})_2(NCS)_2^+$.[23]

The dihedral angles between the plane of the pyridine ring and the C═O bond of the corresponding ester group are 7.6 and 13.1°, respectively. These relatively coplanar arrangements, likely affected by the proximity and orientation of the neighboring $I_3^-$ atom, have been theoretically predicted to influence the overlap of the pyridine and carbonyl $\pi$ orbitals.[24]

Triiodide studies in fluid solution are complicated somewhat by the well-known equilibrium shown in eq 3.

(21) Devonshire, R.; Weiss, J. J. *J. Phys. Chem.* **1968**, *72*, 3815−3820.
(22) Grossweiner, L. I.; Matheson, M. S. *J. Phys. Chem.* **1957**, *61*, 1089−1095.
(23) Walter, B. J.; Elliott, C. M. *Inorg. Chem.* **2001**, *40*, 5924−5927.
(24) Persson, P.; Lunell, S.; Ojamae, L. *Chem. Phys. Lett.* **2002**, *364*, 469−474.

$$I^- + I_2 \rightleftharpoons I_3^- \quad (3)$$

Literature values for the equilibrium constant in dichloromethane are very large, $K = 10^5$ $M^{-1}$.[25] Therefore, the initial triiodide concentrations are approximately the equilibrium concentrations under the conditions investigated. The slight red-shift in the absorption spectrum of $Ru(bpy)_2(deeb)^{2+}$, observed at high $I_3^-$ concentrations, could be accounted for by ion pairing with iodide, as previously described.[11] However, the magnitude of the quenching constants, and our inability to see charge-separated products, clearly indicate that the excited-state quenching behavior reported here is not caused by iodide.[11]

The strongest evidence for ion pairing between $Ru(bpy)_2(deeb)^{2+}$ and $I_3^-$ was the appearance of a static component in the time-resolved photoluminescence quenching. The number of excited states observed after laser excitation decreased with increasing triiodide concentration. In addition, the upward curvature in the Stern−Volmer plots of the steady-state PL in dichloromethane supports the presence of both static and dynamic quenching.[19] Excited states that are quenched by both static and dynamic quenching can be described by eq 4

$$\frac{PLI_0}{PLI} = 1 + (K_D + K_S)[I_3^-] + K_D K_S [I_3^-] \quad (4)$$

where $[I_3^-]$ is the equilibrium triiodide concentration and $K_D$ and $K_S$ are the dynamic and static quenching constants, respectively.[19] A reasonable fit to the steady-state photoluminescence data was generated using eq 4 and the quenching constants, $K_D$ and $K_S$, determined from time-resolved emission, Figure 2A inset. The agreement between the experimental and simulated data in the Figure 2A inset demonstrates that the time-resolved and steady-state quenching are reporting on the same fundamental process.

The static component was attributed to the formation of the ground-state adduct between $Ru(bpy)_2(deeb)^{2+}$ and $I_3^-$ with an equilibrium constant $K_s = 51{,}000$ $M^{-1}$ (eq 5).

$$Ru^{II}(bpy)_2(deeb)^{2+} + I_3^- \rightleftharpoons [Ru^{II}(bpy)_2(deeb)^{2+},(I_3^-)]^+ \quad (5)$$

Significant dynamic quenching was also observed, with a calculated $K_D = 54\,000$ $M^{-1}$. While some laser scattering by the $TiO_2$ thin films made small amplitude changes difficult to detect, there was no experimental evidence for static quenching of $Ru^{2+}*/TiO_2$ in dichloromethane solution. Efficient dynamic quenching was observed with $K_D = 40{,}000$ $M^{-1}$, which corresponds to a bimolecular rate constant remarkably similar to that measured in fluid solution, $k_q = 3.6 \times 10^{10}$ $M^{-1}$ $s^{-1}$. Excited-state quenching was purely dynamic in acetonitrile and is summarized in Table 1.

Nanosecond transient-absorption experiments detected the MLCT excited states of $Ru(bpy)_2(deeb)^{2+}*$ and $Ru^{2+}*/TiO_2$. However, no reaction products resulting from the excited-state quenching were observed. As a result, discussions of the excited-state relaxation pathways in the presence of $I_3^-$ remain largely speculative. Previous literature has shown that MLCT excited states are often quenched by energy transfer, reductive electron transfer, or oxidative electron transfer.[10,26,27] Equations 6−8 give the expected products of such reactions with triiodide.

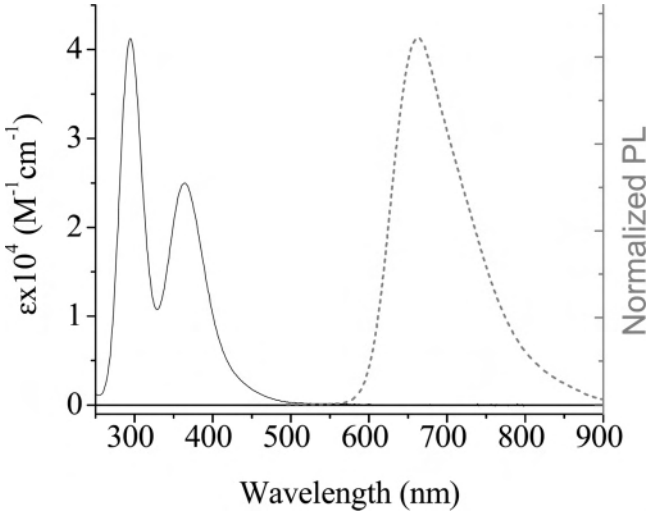


**Figure 7.** UV−vis absorption spectrum of $TBAI_3$ (−) plotted against an area-normalized emission spectrum for $Ru(bpy)_2(deeb)^{2+}*$ (···) in $CH_2Cl_2$.

$$Ru^{III}(bpy)_2(deeb^-)^{2+*} + I_3^- \rightarrow Ru^{II}(bpy)_2(deeb)^{2+} + I_3^-* \quad (6)$$

$$Ru^{III}(bpy)_2(deeb^-)^{2+*} + I_3^- \rightarrow Ru^{II}(bpy)_2(deeb^-)^{+} + I_3^{\bullet} \quad (7)$$

$$Ru^{III}(bpy)_2(deeb^-)^{2+*} + I_3^- \rightarrow Ru^{III}(bpy)_2(deeb)^{3+} + I_3^{2-} \quad (8)$$

Energy transfer would yield $I_3^-*$ (eq 6). Triiodide excited states are known, and room-temperature emission in ethanol has been reported.[28,29] We were unable to observe $I_3^-*$ emission with direct 355 nm excitation of $I_3^-$ in dichloromethane or acetonitrile solutions in either the presence or absence of ruthenium compounds. Such excitation did yield $I_2^{-\bullet}$ as has been previously reported.[22] Efficient energy transfer requires spectral overlap between the ground-state absorption of the acceptor ($I_3^-$) and the photoluminescence spectrum of the donor ($Ru(bpy)_2(deeb)^{2+}*$).[30] However, as shown in Figure 7, there was negligible overlap between these two spectra and energy transfer is therefore an unlikely explanation for the efficient quenching observed.

The reductive quenching pathway would result in the formation of $I_3^{\bullet}$, as depicted in eq 7. While $I_3^{\bullet}$ formation has been observed in the gas phase,[31,32] to our knowledge, it has not been reported in solution. Oxidative quenching could yield $I_3^{2-}$ as shown in eq 8 or proceed via a dissociative

(25) Larsen, D. W.; Mestemacher, S. A. *J. Inorg. Nucl. Chem.* **1971**, *33*, 869−874.
(26) Murtaza, Z.; Zipp, A. P.; Worl, L. A.; Graff, D.; Jones, W. E.; Bates, W. D.; Meyer, T. J. *J. Am. Chem. Soc.* **1991**, *113*, 5113−5114.
(27) Crowley, C. E.; Clark, C. D.; Hoffman, M. Z. *Inorg. Chem.* **1998**, *37*, 5704−5709.
(28) Gilch, P.; Hartl, I.; An, Q. R.; Zinth, W. *J. Phys. Chem. A* **2002**, *106*, 1647−1653.
(29) Gershgoren, E.; Banin, U.; Ruhman, S. *J. Phys. Chem. A* **1998**, *102*, 9−16.
(30) Förster, T. *Modern Quantum Chemistry*, Vol. III; Academic Press: New York, 1965.

electron-transfer mechanism to produce $I_2^{-\bullet}$ and $I^-$. To our knowledge, no spectroscopic evidence exists for either of these pathways. However, it is a likely mechanism for the cathodic photocurrents recently reported.[14] While no cathodic photocurrents were observed in this study, the excited state was efficiently quenched. If the quenching were based on oxidative or reductive electron transfer, our inability to spectroscopically observe the products suggests that the cage-escape yields were very low ($\phi_{ce} < 0.1$) in acetonitrile, dichloromethane, and for the sensitizers bound to $TiO_2$.

Unfortunately, the $I_3^{\bullet/-}$ and $I_3^{-/2-}$ reduction potentials are not easily estimated by cyclic voltammetry as the more facile $2e^-$ reduction waves are observed.[33] For example, in acetonitrile electrolyte, we observed two $2e^-$ reductions by rotating disk electrochemistry assigned to the oxidations of $I^-$ and $I_3^-$.[34] These $2e^-$ reduction potentials are highly unlikely to be relevant to the MLCT excited-state quenching results observed here. The relevant excited state reduction potentials, on the other hand, are easily estimated in fluid solution and for sensitizers anchored to $TiO_2$.[34] Future studies with a larger number of ruthenium polypyridyl compounds whose MLCT excited states span a large potential range would allow the $I_3^-$ reduction potential to be determined.

## Conclusions

The excited states of $Ru(bpy)_2(deeb)^{2+}$ efficiently quenched by triiodide ($I_3^-$) in dichloromethane and anchored to $TiO_2$. In dichloromethane, $I_3^-$ was found to quench the excited states by static and dynamic mechanisms. Stern−Volmer analysis produced self-consistent data between time-resolved and steady-state photoluminescence measurements that provide an estimate for the $[Ru^{II}(bpy)_2(deeb)^{2+},(I_3^-)]^+$ equilibrium constant, $K_S = 51\,000\ M^{-1}$. For studies performed on $TiO_2$, dynamic quenching was observed with a bimolecular rate constant $k_q = 3.6 \times 10^{10}\ M^{-1}\ s^{-1}$. X-ray crystallographic, IR, and Raman data gave evidence for interactions between $I_3^-$ and the bpy and deeb ligands in the solid state. The results suggest that under conditions of weak sensitizer-semiconductor electronic coupling, sensitized quenching by $I_3^-$ may compete with electron injection and lower the solar-energy conversion efficiency of DSSCs.

**Acknowledgment.** The Division of Chemical Sciences, Office of Basic Energy Sciences, Office of Energy Research, U.S. Department of Energy is gratefully acknowledged for research support.

**Supporting Information Available:** Crystallographic data in CIF format. This material is available free of charge via the Internet at http://pubs.acs.org.

IC060246Q

(31) Taylor, T. R.; Asmis, K. R.; Zanni, M. T.; Neumark, D. M. *J. Chem. Phys.* **1999**, *110*, 7607−7609.
(32) Choi, H.; Taylor, T. R.; Bise, R. T.; Hoops, A. A.; Neumark, D. M. *J. Chem. Phys.* **2000**, *113*, 8608−8614.
(33) Macagno, V. A.; Giordano, M. C.; Arvia, A. J. *Electrochim. Acta* **1969**, *14*, 335−357.
(34) Bergeron, B. V.; Marton, A.; Oskam, G.; Meyer, G. J. *J. Phys. Chem. B* **2005**, *109*, 937−943.